International Journal of GEOMATE, Jan., 2023, Vol.24, Issue 101, pp.102-109
ISSN: 2186-2982 (P), 2186-2990 (O), Japan, DOI: https://doi.org/10.21660/2023.101.g12251
Geotechnique, Construction Materials and Environment

FRAGILITY CURVE OF SCHOOL BUILDING IN PADANG CITY WITH AND WITHOUT RETROFITTING DUE TO EARTHQUAKE AND TSUNAMI LOADS

*Fauzan[1], Ruddy Kurniawan[2], Nandaria Syahdiza[3], Zev Al Jauhari[4] and Dyan Adhitya Nugraha M[5]

[1,2,3,5]Engineering Faculty, Andalas University, Indonesia; [4]Department of Civil Engineering, Bengkalis Polythecnic, Indonesia

*Corresponding Author, Received: 21 Sep. 2022, Revised: 16 Dec. 2022, Accepted: 11 Jan. 2023

ABSTRACT: SMPN 25 building in Padang City is a junior high school building located in the high seismic zone and prone to tsunamis. Based on the initial analysis of the existing building using the current Indonesian building codes, this building has not been able to withstand the working earthquake and tsunami loads. In this study, the retrofitting of the building was designed using concrete jacketing that is with additional dimensions and reinforcement, aimed at making the building function as a vertical evacuation structure. The structural fragility curve of the building is determined before and after retrofitting for both earthquake and tsunami loads. The fragility curve is determined from the ductility of the building for each variation of earthquake acceleration based on the Hazus standard. The first yield displacement was determined from the pushover analysis, and the ultimate displacement was determined from the time history analysis. The earthquake acceleration records used were the El-Centro earthquake, the Northridge earthquake, the Kobe earthquake, and the Padang earthquake. The results of the analysis show that the retrofit of the building structure using concrete jacketing reduces the probability of damage to the building structure due to earthquake loads by 42.06% at the level of extensive damage and by 4.42% at the level of complete damage at PGA 0.6g, while, it reduces the probability of building damage due to tsunami loads by 45.53% at the level of extensive damage and by 26.32% at the level of complete damage at a tsunami inundation depth of 4.5m.

Keywords: Fragility curves, School building, Tsunami loads, Earthquake, Retrofit

1. INTRODUCTION

Indonesia has experienced big seismic triggered disasters in terms of earthquakes and tsunamis. West Sumatra Province is an area prone to earthquakes and tsunamis in Indonesia. The tsunami disaster hit West Sumatra in Siberut (1797) and Sipora-Pagai, Mentawai Island (1833), West Sumatra Province, Indonesia. These two tsunamis had different effects in terms of time to reach and inundation height [1].

McCloskey et al. [2] stated that the time interval between the occurrence of the first strong earthquake and the onset of the tsunami that hit the Padang coast was about 20-30 minutes. Based on the earthquake inundation map in Padang City, people must save themselves with a distance of 3-5 km to get safe area. It is estimated that the community does not have enough time to evacuate horizontally, so it will be more effective to evacuate vertically [3].

Vertical evacuation must be supported by a strong building structure that is resistant to earthquake and tsunami loads. In addition to the structure of the building must be strong enough to withstand earthquake loads that occur, the building must be able to withstand the load caused by the tsunami wave [3].

Padang City, the capital city of West Sumatra, is located along the west coast of Sumatra. It is located near the border of the Eurasia and Indo-Australia plates, resulting in Padang City as one of the cities with a high risk of earthquake and tsunami (vulnerable to tsunami hazards). SMPN 25 building in Padang City is located in the tsunami red zone area.

An analysis of the existing building of SMPN 25 Padang based on the current Indonesian seismic standard (SNI 1726-2019) [4] and tsunami loads (FEMA P-646-508) [5] had been carried out which aims to investigate the ability of the building structure to withstand a combination of earthquake and tsunami loads. The results obtained from the structural analysis of the existing building show that several structural elements are not able to withstand the tsunami loads acting on the building structure, so it is necessary to design the retrofit of the building structure, so that the building can be used as a tsunami vertical evacuation.

To estimate the probability of structural damage to the building, a fragility curve of the school building with and without retrofitting due to earthquake and tsunami loads was developed in this study.

2. RESEARCH SIGNIFICANCE

This study provides seismic and tsunami fragility curve for RC school building structures before and after retrofitting that has been developed with various ground motion data of earthquake loads and inundation depth of tsunami loads in Padang City, Indonesia. A fragility curve is a relationship between the damage state and the intensity of natural hazards. In this study, the finding of fragility curves can be used to predict the damage probability of a school building under an earthquake or tsunami hazard and to develop risk management strategies.

3. ANALYSIS OF THE STRUCTURE

3.1 Structural Modelling

SMPN 25 building is an existing building in Padang City which is located in a tsunami inundation area, around 0.97 km from the coastal line (Fig.1). The building is located on Beringin Raya Street, Lolong Belanti, North Padang, Padang City, West Sumatra, with coordinates latitude -0.919197 and longitude 100.357238. The building is a four-story reinforced concrete (RC) structure with a 15m height. Table 1 shows the details of the SMPN 25 Padang building.

In this study, the building structure was modeled with and without retrofitting using ETABS v.18. 3D modeling and plans of building structures are shown in Figs.2 and 3.

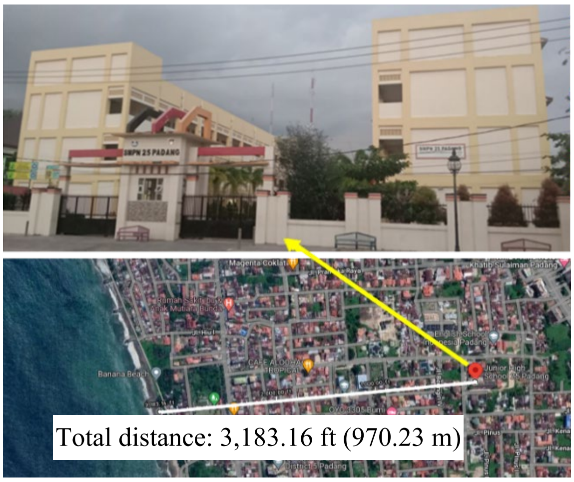

Fig.1 The front view and the location of the SMPN 25 building in Google Earth software

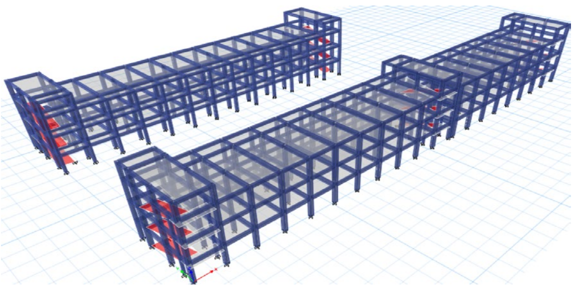

Fig.2 The 3-D modeling of the SMPN 25 building using ETABS software

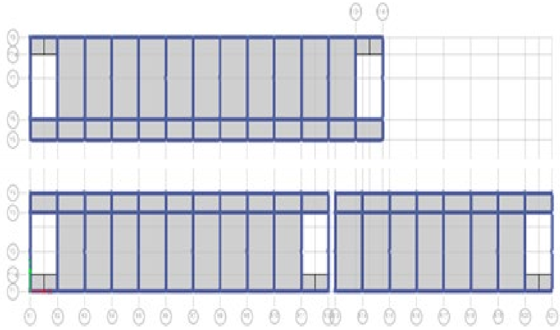

Fig.3 The plan view of the SMPN 25 Padang building

Table 1 Details of SMP N 25 Padang building

	Beam		Column		
	Code	Dimension (cm)	Code	Dimension (cm)	Main Bars (mm)
Tie Beam	S1	35x70			
	S2	35x70			
	S3	35x70			
Story 1	1B1	30x70	1K1	45x45	12D22
	1B2A	30x70	1K1A	45x45	16D22
	1B2	30x55	1K2	35x40	12D22
	1B3	30x50	1K3	35x35	12D22
Story 2	2B1	30x70	2K1	45x45	8D22
	2B2A	30x70	2K1A	45x45	12D22
	2B2	30x50	2K2	35x40	8D22
	2B3	30x45	2K3	35x35	8D22
Story 3	3B1	30x70	3K1	45x45	8D22
	3B2A	30x70	3K1A	45x45	8D22
	3B2	30x50	3K2	35x40	8D22
	3B3	30x45	3K3	35x35	8D22
Pent House	4B2	30x50	4K1	45x45	8D19
	4B3	30x45	4K2	35x40	8D19
			4K3	35x35	4D19
Stair	BT	25x30	KT	25x25	4D16

3.2 Loading Analysis

3.2.1 Gravity load

The gravity loads used in this study are live load, dead load, and wall load based on SNI 1727-2020 [6] and SNI 2847-2019 [7] and refugee load based on FEMA P-646-508-2019.

3.2.2 Earthquake load

The response spectrum based on SNI 1726-2019 was used as the earthquake load for the building analysis with and without retrofitting. Meanwhile, the ground motion earthquake data (time history) for non-linear time history analysis was used as an engineering demand parameter (EDP) in the calculation of the fragility curve. In this study, the earthquake ground motion data uses four earthquake ground motion recording data, as shown in Table 2. Each ground motion earthquake data is matched with the earthquake characteristics of Padang City for medium soil types using Seismomatch software. Each earthquake ground motion data is scaled with a variation of 0.2 to 2.0 with an interval of 0.2.

Table 2 Earthquake peak ground acceleration data

Earthquake	Original PGA	PGA matched
El-Centro 1940	0.36 g	0.63 g
Northridge 1994	0.60 g	0.76 g
Kobe 1995	0.34 g	0.60 g
Padang 2009	0.60 g	0.60 g

3.2.3 Tsunami loads

The tsunami loads and load combinations due to tsunami were calculated based on the FEMA P-646-508 2019 with an inundation depth of 4.5 m based on the inundation map of Padang City. In this study, the calculation result of the tsunami loads on the building structure is hydrostatic force (49.17 kN), buoyant force (5.40 kN/m^2), hydrodynamic force (12.95 kN), impulse force (19.42 kN), debris impact loads (200.72 kN), debris damming effects (1,311.11 kN), uplift force (0.001 kN/m^2), and additional gravity loads (5.40 kN/m^2). These loads are applied to structural components such as columns and slabs.

3.3 Analysis of Existing Building

The analysis of the existing building includes examining the cross-sectional capacity of the column and beam elements of the building against earthquake loads and combined earthquake and tsunami loads acting on the structure [8].

Based on the analysis of the existing building of SMPN 25 Padang building against earthquake and tsunami loads, several structural elements have not been able to withstand the tsunami loads such as the 2nd floor columns and the 1st floor beams. The structural elements that have not been able to withstand the tsunami loads are shown in Fig.4.

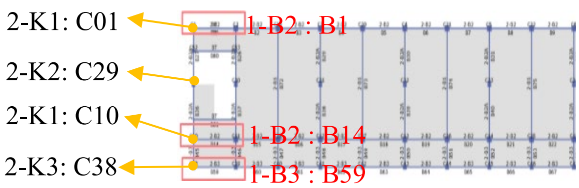

Fig.4 Structural elements that have not been able to withstand the tsunami loads

3.4 Structural Retrofitting

One of the alternatives designed for the retrofitting building against tsunami loads is the concrete jacketing method which is enlarging the column cross-section and adding flexural and shear reinforcement of the column around the old column [9,10]. In this study, retrofitting using concrete jacketing was designed for several structural elements in the building structure which have not been able to carry the load acting on the building structure due to the addition of the tsunami loads.

Retrofitting design using concrete jacketing on weak structural elements was carried out based on the results of existing building analysis and the minimum requirements for adding dimensions and reinforcement for jacketing.

Tables 3 and 4 show the dimensions and details of the existing and retrofitted structural elements. Figures 5 and 6 show the cross-sectional dimension and the modeling of the retrofitted building structure.

The analysis of the flexural cross-sectional capacity of the existing building structure can be observed in the axial-flexural (P-M) interaction diagram of the column (Fig.7). Table 5 shows the shear capacity of the existing building column. The beam flexural cross-sectional capacity is shown in Table 6.

Table 3 Existing column dimensions of the SMPN 25 Padang building

Story	Existing columns			
	Column type	Dimension (cm)	Ø (mm)	Reinforcement bar
Story 1	1-K1 (C01)	45x45	22	12
	1-K2 (C29)	45x35	22	12
	1-K3 (C38)	35x35	22	12
Story 2	2-K1 (C01)	45x45	22	8
	2-K2 (C29)	45x35	22	8
	1-K3 (C38)	35x35	22	8

Table 4 Concrete jacketing dimension of the retrofitted SMPN 25 Padang building

Story	Concrete jacketed columns			
	Column type	Dimension (cm)	Ø (mm)	Reinforcement bar
Story 1	1-K1 retrofit (C01)	60x60	22	12
	1-K2 retrofit (C29)	50x60	22	12
	1-K3 retrofit (C38)	50 x50	22	12
Story 2	2-K1 retrofit (C01)	60x60	22	12
	2-K2 retrofit (C29)	50x60	22	12
	2-K3 retrofit (C38)	50x50	22	12

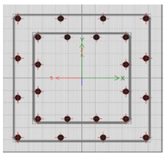

(a) 1-K1 retrofit: C01 Dimension 600x600mm

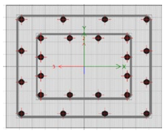

(b) 1-K2 retrofit: C29 Dimension 500x600mm

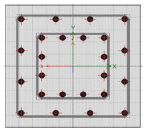

(c)1-K3 retrofit: C38 Dimension 500x500 mm

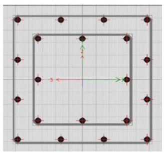

(d) 2-K1 retrofit: C01Dimension 600x600mm

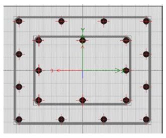

(e) 2-K2 retrofit: C29Dimension 500x600 mm

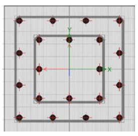

(f) 2-K3 retrofit: C38Dimension 500x500 mm

Fig.5 Steel reinforcement details of the concrete jacketed columns

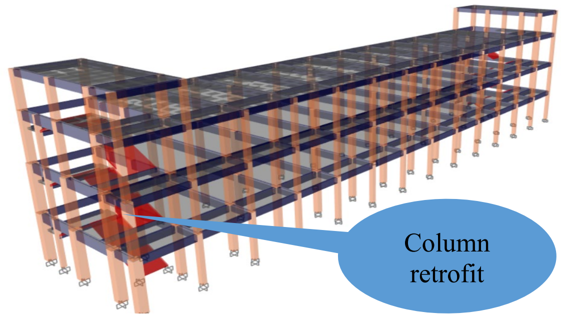

Fig.6 The 3-D modeling of the retrofitted SMPN 25 Padang building with concrete jacketing

3.5 Load Bearing Capacities of Structure with and without Retrofitting

The P-M interaction diagram is used to describe the capacity of the column to withstand the working loads. Figure 7 shows the comparison of the P-M interaction diagram obtained from the results of the structural analysis of the building with and without retrofitting. From the figure, it can be recognized that retrofitting columns improves the capacity of the building structure, in which columns of the retrofitted building have been able to withstand tsunami loads acting on the structure. The comparison of the shear capacity of the column with and without retrofit is shown in Table 5. As can be seen from the table, the shear capacity of the columns improves after the retrofitting, in which the beam shear capacity of the retrofitted building can resist the applied working loads including tsunami loads.

The comparison of the flexural capacity of the beam with and without retrofit is shown in Table 6. As seen in the table that retrofitting columns improves the capacity of the beam, so the beams can withstand the tsunami loads. From this analysis, the beam shear capacities are also able to withstand tsunami loads.

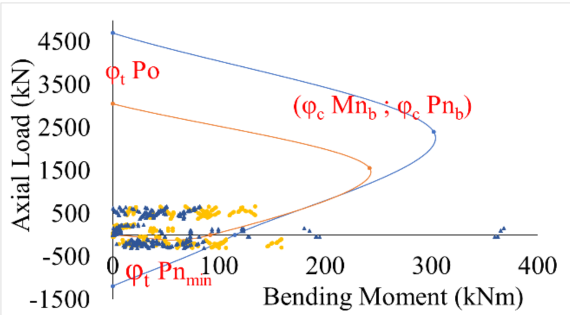

(a) Column without retrofit (2-K1:C1)

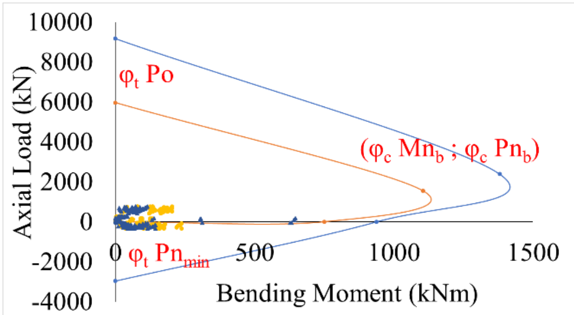

(b) Column with retrofit (2-K1 retrofit:C1)

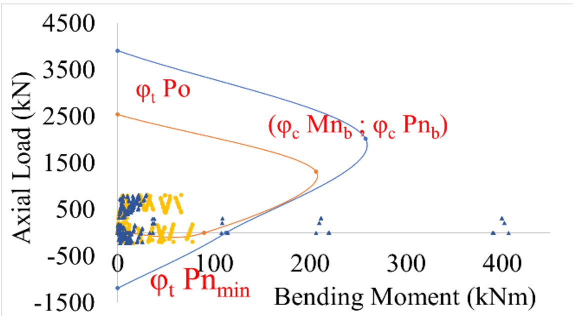

(c) Column without retrofit (2-K2:C29)

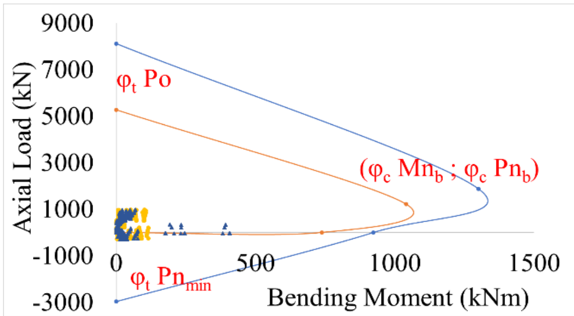

(d) Column with retrofit (2-K2 retrofit:C29)

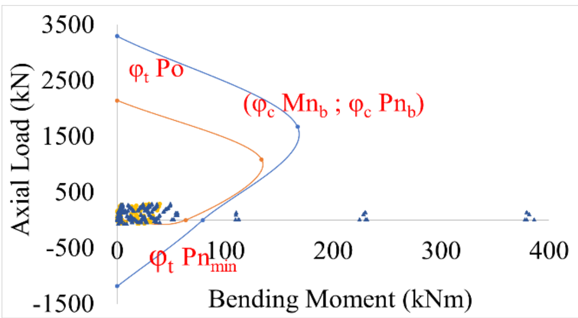

(e) Column without retrofit (2-K3:C38)

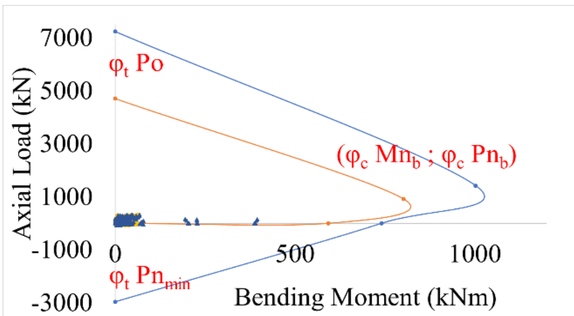

(f) Column with retrofit (2-K3 retrofit:C38)

Fig.7 P-M interaction diagram of the 2nd floor column with and without retrofitting

Table 5 Comparison of the shear capacity of the columns with and without retrofitting

Without retrofitting						With retrofitting					
Column Section	Code	Shear reinforcement	Vr (kN)	Vu' (kN)	Vu ≤ Vr	Column Section	Code	Shear design reinforcement	Vr (kN)	Vu' (kN)	Vu ≤ Vr
2-K1 (45x45)	C01	Ø10-100 mm	293.43	1037.01	Not Ok	2-K1 retrofit (60x60)	C01	Ø13-50 mm	1060.98	1037.01	Ok
2-K2 (45x35)	C29	Ø10-100 mm	270.09	1180.61	Not Ok	2-K2 retrofit (60x50)	C29	Ø16-50 mm	1476.79	1180.61	Ok
2-K3 (35x25)	C38	Ø10-100 mm	204.21	1185.72	Not Ok	2-K3 retrofit (50x50)	C38	Ø16-50 mm	1213.08	1185.72	Ok

Table 6 Comparison of the flexural capacity of the beams with and without retrofitting

Beam		The number of reinforcements		φMn	Without retrofitting			With retrofitting		
Section	Code	Tens.	Comp.	(kNm)	Mu (kNm)		Mu ≤ Mn	Mu (kNm)		Mu ≤ Mn
1-B2 30/55	B01	3D19	3D19	119.09	170.89	P	Not Ok	115.26	P	Ok
		3D19	3D19	119.09	120.99	M	Ok	58.83	M	Ok
1-B2 30/55	B14	3D19	3D19	119.09	175.8	P	Not Ok	115.26	P	Ok
		3D19	3D19	119.09	85.21	M	Ok	58.83	M	Ok
1-B3 30/70	B59	3D19	3D19	106.65	197.19	P	Not Ok	106.06	P	Ok
		3D19	3D19	106.65	120.86	M	Ok	66.59	M	Ok

4. FRAGILITY CURVE DEVELOPMENT

The fragility curve is a log-normal function that describes the probability of exceeding certain structural damage conditions by taking into account irregularities related to capacity, demand, and damage conditions [11]. The fragility curve depicts the relationship between the probability of the degree of structural damage and the hazard intensity measure.

In this study, an analytical method was carried out to obtain the fragility curve of the building with and without retrofitting due to earthquake and tsunami loads. Analytical fragility curve developed from structural response and capacity.

The development of the fragility curve was carried out based on the Hazus standard [11,12], and it was developed using the probabilistic seismic demand model (PSDM) method with a cloud approach.

The PSDM is a mathematical relation between hazard intensity measure (IM) and structural response as an engineering demand parameter (EDP). The cloud approach method was used in this study by doing regression analysis between IM and EDP with uncertainty variables a and b [13].

The general equation for the development of the fragility curve is shown in Eq. (1).

$$\mathbf{Fragility = P\ [LS][IM] = y} \qquad (1)$$

Where LS is the boundary condition or damage condition (DS), IM is the intensity measure of hazard, and y is the state reached due to the intensity measure (IM).

The equation is then idealized into a log-normal distribution, as shown in Eq. (2).

$$\mathbf{P(x)} = \Phi\left[\frac{\ln(x)-\lambda}{\zeta}\right] \qquad (2)$$

Where P(x) is a probability function, x is a random variable, ζ is the standard deviation value of ln x, λ is the mean value of ln x, and Φ is the form of the cumulative normalized distribution. Log-normal is used because it is very suitable to determine various types of damage ranging from failure of structural components, non-structural components, building collapse, and the probability of zero on EDP equal to zero and below zero.

In this study, there are two types of fragility curves developed, namely seismic fragility curve with and without retrofitting and tsunami fragility curve with and without retrofitting. Figure 8 shows the fragility curve development flowchart in this study.

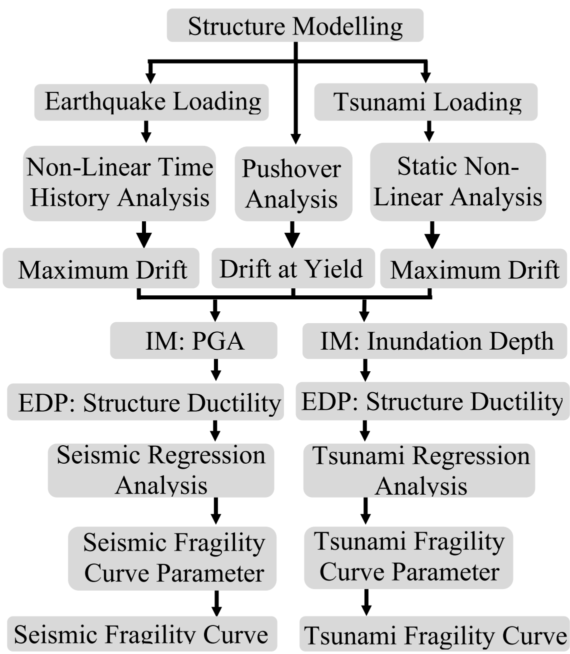

Fig.8 Fragility curve development flowchart

4.1 Seismic Fragility Curve

The seismic fragility curve depicts the relationship between the probability of the degree of structural damage and the ground motion intensity measure (IM). The IM used in the seismic fragility curve is peak ground acceleration (PGA).

The parameters used in the calculation of the seismic fragility curve are obtained from the results of pushover analysis in the form of drift yield values and from the results of non-linear time history analysis in the form of maximum drift values [13-15].

4.1.1 Pushover analysis

The capacity curve from the pushover analysis illustrates the relationship between base shear and rooftop displacement. In this study, the capacity curve from the pushover analysis is used to check the performance level of the existing structure and functions as an engineering demand parameter (EDP) in the calculation of the building fragility curve with and without retrofitting which is given through the drift yield value.

There are three methods used to determine displacement yield, namely the first yield is based on the first yield deviation that occurs, the significant yield is based on the intersection between the elastic displacement and the equivalent load at the time of failure, and the same energy absorption capacity between the elastoplastic system with the actual structure at the same ultimate load. In this study, a significant yield was used to determine the displacement yield value of the fragility curve.

4.1.2 Non-linear time history analysis

In this study, the non-linear time history analysis uses four types of ground motions earthquake data (earthquake El-Centro, Northridge, Kobe, and Padang) which are scaled on a 0.2–2.0 scale with an interval of 0.2. So, there are 40 ground motion data used in the calculation of the seismic fragility curve. The non-linear time history analysis result is used as the engineering demand parameter (EDP) to develop the fragility curve with maximum drift value.

4.1.3 Seismic ductility of the structure

The ductility of the structure used in this study is generated as regression analysis data to be a fragility curve parameter. The ductility of the structure can be calculated by dividing each maximum drift value from the non-linear time history analysis result by the drift yield value from the pushover analysis result.

4.1.4 Seismic regression analysis

Regression analysis in this study aims to obtain the uncertainty variable (a and b). Regression analysis was performed between the value of the intensity measure (IM) on the X-axis and the value of the engineering demand parameter (EDP) on the Y-axis.

4.1.5 Development of seismic fragility curve

The general equation for the development of the seismic fragility curve is shown in Eq. (2). The equation is idealized into a log-normal distribution.

4.2 Tsunami Fragility Curve

The tsunami fragility curve depicts the relationship between the probability of the degree of structural damage and the tsunami intensity measure (IM). The tsunami intensity measure used in this study is tsunami inundation depth (m).

In this study, an inundation map of Padang City was used to develop a tsunami fragility curve using various inundation depths (0.5 m – 5 m) with intervals of 0.5 m.

The parameters used in the calculation of the tsunami fragility curve are obtained from the result of static non-linear analysis in the form of maximum drift values.

The development of the tsunami fragility curve in this study is adapted from the earthquake fragility curve development. The general equation for the development of the tsunami fragility curve is shown in Eq. (2) that idealized into a normal distribution.

Statical parameters of fragility function λ and ζ are obtained by plotting ln x and the inverse of Φ^{-1} on lognormal probability papers and conducting the least-square-fitting of this plot [16].

5. RESULTS AND DISCUSSION

Based on the pushover analysis results, the significant yield value obtained for the existing building was 67.30 mm and that of the retrofitted building was 38.98 mm

The drift yield value used in the fragility curve calculation is obtained from the comparison of the displacement yield value with the building height. Based on the results of the pushover analysis, the drift yield of the building structure is 0.45% and 0.26% for the existing and retrofitted buildings, respectively.

5.1 Seismic Fragility Curve Result

The parameters for seismic fragility functions obtained from the calculation results are used to describe the seismic fragility curve for the building with and without retrofitting, as shown in Table 7.

Table 7 Parameters for seismic fragility functions

Damage level	Without retrofit		With retrofit	
	λ	ζ	λ	ζ
Slight Damage	-2.55	0.28	-1.99	0.28
Moderate Damage	-1.83	0.28	-1.27	0.28
Extensive Damage	-0.69	0.50	-0.13	0.50
Complete Damage	0.32	0.50	0.89	0.50

Figures 9 and 10 show the seismic fragility curve of the existing building (EX) and retrofitted building (RET), respectively. The tsunami fragility curve is organized into four damaged levels ranging from slight damage to complete damage.

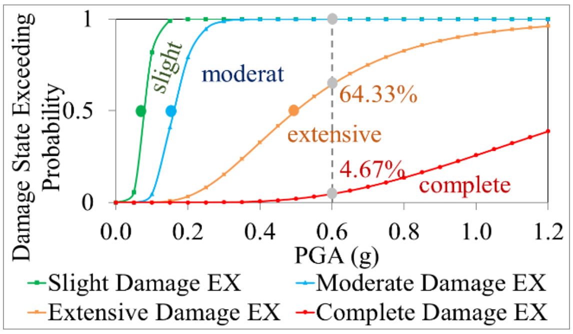

Fig.9 Seismic fragility curve of the existing building

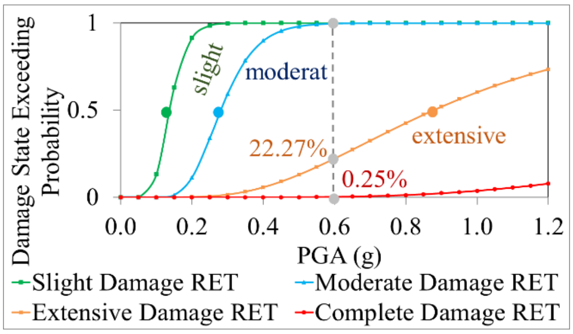

Fig.10 Seismic fragility curve of the retrofitted building

Table 8 shows the probability of damage level of the structural building with and without retrofit during an earthquake with a PGA value of 0.6g.

Table 8 The damage probability percentage of the building with and without retrofit during an earthquake

Damage level	Percentage of probability Without retrofit	Percentage of probability With retrofit	Percentage decrease
Slight Damage	100.00%	100.00%	0%
Moderate Damage	99.99%	99.66%	0.33%
Extensive Damage	64.33%	22.27%	42.06%
Complete Damage	4.67%	0.25%	4.42%

From Figs.9 and 10, it can be seen that the structural damage probability decreases after the building structure was retrofitted. The retrofit of the building structure using concrete jacketing reduces the probability of damage to the building structure by 42.06% at the level of extensive damage and by 4.42% at the level of complete damage at PGA = 0.6g, as shown in Table 8.

5.2 Tsunami Fragility Curve Result

Table 9 shows the parameters for tsunami fragility functions to develop the tsunami fragility curve for the building with and without retrofitting.

Table 9 Parameters for tsunami fragility functions

Damage level	Without retrofit λ	Without retrofit ζ	With retrofit λ	With retrofit ζ
Slight Damage	1.78	0.43	1.72	0.70
Moderate Damage	2.56	0.43	2.92	0.70
Extensive Damage	3.79	0.62	4.70	0.96
Complete Damage	4.89	0.62	6.30	0.96

Based on the parameters for tsunami fragility functions in Table 9, the tsunami fragility curve of the existing (EX) and retrofitted buildings (RET) was obtained, as shown in Figs.11 and 12, respectively.

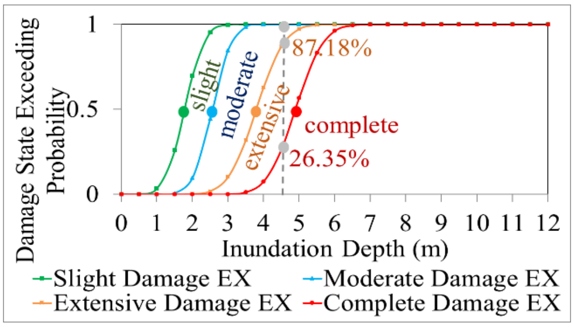

Fig.11 Tsunami fragility curve of the existing building

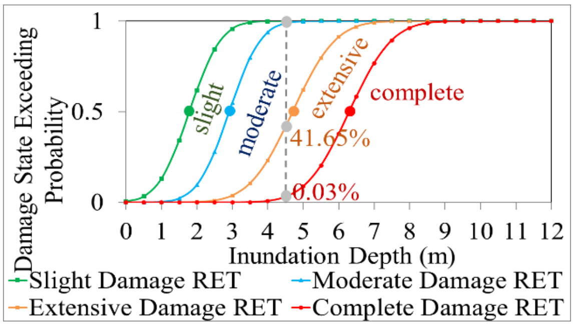

Fig.12 Tsunami fragility curve of the retrofitted building

As can be seen from these figures, the retrofitting of the building structure reduces the damage probability due to tsunami loads. The detailed percentage decrease in damage probability of the existing and retrofitted building with an inundation depth of 4.5 m is shown in Table 10.

Table 10 The damage probability of the building with and without retrofit during a tsunami

Damage level	Percentage of probability Without retrofit	Percentage of probability With retrofit	Percentage decrease
Slight Damage	100.00%	100.00%	0%
Moderate Damage	99.99%	98.80%	1.19%
Extensive Damage	87.18%	41.65%	45.53%
Complete Damage	26.35%	0.03%	26.32%

According to Table 10, the percentage of the structural damage probability for the retrofitted building decreases considerably due to the concrete jacketing column. The percentage decrease of the damage probability due to tsunami loads at an inundation depth of 4.5 m was 45.53% and 26.32% at the level of extensive damage and the level of complete damage, respectively.

6. CONCLUSION

The structure of the SMPN 25 Padang building was modeled with and without retrofit against earthquake and tsunami loads. The results of the existing building analysis show that several columns on the 2nd floor and several beams on the 1st floor have not able to withstand the tsunami loads.

Retrofitting the building using the concrete jacketing method on columns improves the capacity of the building structure, so the building can withstand the tsunami loads.

Based on the fragility curve developed, the percentage of the structural damage probability decreases after the structure was retrofitted. For the seismic fragility curve, the retrofit of the building structure using concrete jacketing reduces the probability of damage to the building structure by 42.06% at the level of extensive damage and by 4.42% at the level of complete damage at earthquake loads with PGA = 0.6g. For the tsunami fragility curve, meanwhile, the retrofit of the building structure reduces the probability of damage to the building structure by 45.53% at the level of extensive damage and by 26.32% at the level of complete damage at a tsunami inundation depth of 4.5 m.

7. ACKNOWLEDGMENTS

The authors gratefully acknowledge the financial support provided by Andalas University.

8. REFERENCES

[1] Borrero J. C., Sieh K., Chlieh M., and Synolakis E., Tsunami Inundation Modeling for Western Sumatra, PNAS, Vol. 103, No. 52, 2006, pp.19673–19677.

[2] McCloskey J., Antonioli A., Piatanesi A., Sieh K., Steacy S., Nalbant S., Cocco M., Giunchi C., Huang J., and Dunlop P, Tsunami threat in the Indian Ocean from a future megathrust earthquake west of Sumatra, Earth and Planetary Science Letters, Vol. 265, 2008, pp.61–81

[3] Ashar F., Amaratunga D., and Haigh R., The Analysis of Tsunami Vertical Shelter in Padang City, in Proc. 4th Int. Con. on Build. Res., Salford Quays, U K, 2014, pp.916-923.

[4] Indonesian National Standardization Agency, Procedures for Planning Earthquake Resistance for Building and Non-Building Structures SNI 1726-2019, BSN, Jakarta, 2019, pp.1-248.

[5] Federal Emergency Management Agency, FEMA P646: Guidelines for Design of Structure for Vertical Evacuation from Tsunami 2nd edition, FEMA, California, 2012, pp.1-174.

[6] Indonesian National Standardization Agency, Minimum Load for Planning of Buildings and Other Structures SNI 1727:2020, BSN, Jakarta, 2020, pp.1-302.

[7] Indonesian National Standardization Agency, Structural Concrete Requirements for Buildings SNI 2847:2019, BSN, Jakarta, 2019, pp.1-365.

[8] Fauzan, Ismail F. A., Siregar N. and Jauhari Z. A., The Effect of Tsunami Loads on Pasar Raya Inpres Block III Building in Padang City Based on FEMA P-646, in Proc. MATEC Web of Conferences Vol. 258, No. 03020, 2019, pp.1-9.

[9] Fauzan, Ismail F. A., and Jauhari Z. A., Seismic Retrofitting Analysis Using Concrete Jacketing and Shear Wall on Dental Hospital Building of Andalas University, IOP Conf. Series: Materials Sci. Eng., Vol. 602, No. 012108, 2019, pp.1-11.

[10] Fauzan, Ismail F.A., Apriwelni S., Faradiza I., and Jauhari Z. A., Strengthening of Nurul Ilmi Mosque with Concrete Jacketing, INSIST, Vol. 1, No. 1, 2016, pp.25-29.

[11] HAZUS, Earthquake Loss Estimation Methodology, Federal Emergency Management Agency, Washington D. C., 2002, pp.11-21.

[12] HAZUS, Tsunami Model Technical Guidance, Washington, Federal Emergency Management Agency, Washington D.C., 2017, pp. 1-171.

[13] Utami A. C., Kurniawan R., and Fauzan, Analytical Fragility Curve Development of Maternity and Children's M. Djamil Hospital Building Padang due to Earthquake and Tsunami, IOP Conf. Series: Earth and Env. Sci., Vol. 708, No. 012014, 2021, pp.1-10.

[14] Janpila A., Foytong P., Tirapat S., Twhanasisathit N., and Ruangrassamee A., The Optimal Method for Building Damage Fragility Curve Development, Int. Journal of GEOMATE, Vol. 18, Issue 69, 2020, pp. 74-80.

[15] Juliafad E. and Gokon H., Seismic Fragility Function for Single Storey Masonry Wall RC Building in Padang City, Int. Journal of GEOMATE, Vol. 22, Issue 94, 2022, pp.39-46.

[16] Koshimura S., Namegaya Y., and Yanagisawa H., Tsunami Fragility: A New Measure to Identify Tsunami Damage, Journal of Disaster Research, Vol. 4, No. 6, 2009, pp.479-488.